ACS OMEGA

http://pubs.acs.org/journal/acsodf

Article

Effects of Low-Level Gamma Radiation on Common Nitroaromatic, Nitramine, and Nitrate Ester Explosives

Patricia L. Huestis, Jamie A. Stull, Joseph P. Lichthardt, Maryla A. Wasiolek, Lori Montano-Martinez, and Virginia W. Manner*

Cite This: *ACS Omega* 2022, 7, 2842−2849

Read Online

ACCESS | Metrics & More | Article Recommendations | Supporting Information

ABSTRACT: The aging of high explosives in an ionizing radiation field is not well understood, and little work has been done in the low dose and low dose rate regime. In this study, four explosives were exposed to low-level gamma irradiation from a ^{137}Cs source: PETN, PATO, and PBX 9501 both with and without the Irganox 1010 stabilizer. Post-irradiation analysis included GC−MS of the headspace gas, SEM of the pellets and powder, NMR spectroscopy, DSC analysis, impact sensitivity tests, and ESD sensitivity tests. Overall, no significant change to the materials was seen for the dose and dose rate explored in this study. A small change in the ^{1}H NMR spectrum of PETN was observed and SEM and ESD results suggest a surface energy change in PATO, but these differences are minor and do not appear to have a substantial impact on the handling safety.

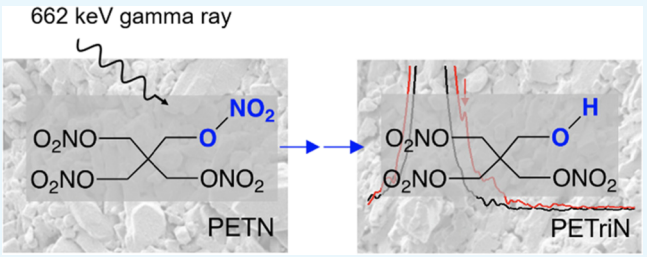

INTRODUCTION

The effects of ionizing radiation on the degradation of high explosives (HEs) are not well understood, especially in the context of the low dose, low dose rate aging conditions encountered in stockpile, or space-based environments. Radiation fields in the stockpile are created by the radioactive decay of ^{239}Pu or ^{235}U, both of which have a long half-life and thus result in a relatively low dose rate environment. Explosives are extensively employed on space shuttles to initiate a variety of pyromechanisms such as component separation and parachute deployment since explosives can generate the necessary impulse without adding much weight to the payload.[1−3] Once the space shuttle is beyond the Earth's magnetosphere, it and everything onboard will then be exposed to larger ionizing radiation fields than those on Earth[4] though these dose rates are similarly modest in comparison to other radiation application environments. A number of studies focused on the radiation aging of HEs have been conducted,[5−18] but their relevance to natural aging conditions is uncertain as both the dose and dose rate can have an effect on the radiation aging of materials. Although this study also utilizes an accelerated dose rate with respect to natural aging conditions, it is the lowest dose rate reported in any published literature thus far. Overall, this study fills a long overdue gap in knowledge on the effects of lower dose radiation aging of explosives and is critical in order to establish handling safety after exposure to ionizing radiation fields.

Ionizing radiation ionizes molecules as it travels through a medium. These ionizations can drive chemistry far from equilibrium, and the resulting chemistry is not always intuitive. Solid-state reactions are particularly difficult to predict and model though general trends are observed. For materials that contain a large fraction of hydrogen (organics), for instance, ionizing radiation is expected to produce a significant amount of hydrogen gas (H_2).[19,20] The process of forming H_2 gas creates radical species on the parent molecule, and these radical species will often react. In the case of solid polymers, irradiation can lead to chain breakage and cross-linking, which can change the material properties in undesirable ways. Polymer binders and plasticizers used in explosive formulations provide stability and strength to pressed shapes; thus, degradation in the polymer system could adversely affect the desired formulation characteristics. Studies on the irradiation of pressed plastic-bonded explosive (PBX) cylinders showed up to a 0.6 g/cm^3 decrease in density after receiving a dose of 2.4 MGy.[5] Even small changes in density or porosity will affect the mechanical and performance properties of HEs.[21,22] The HE itself is also subject to degradation upon irradiation, so it is important to study the radiation effects of HEs and explosive formulations as they are used in order to truly understand the consequences of radiation aging.

For this study, four explosives were chosen: pentaerythritol tetranitrate (PETN), 3−picrylamino−1,2,4−triazole (PATO),

Received: October 12, 2021
Accepted: December 9, 2021
Published: January 10, 2022

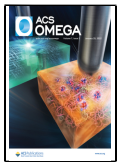

https://doi.org/10.1021/acsomega.1c05703
ACS Omega 2022, 7, 2842−2849

and 1,3,5,7-tetranitro-1,3,5,7-tetrazoctane (HMX)-based PBX 9501, both with and without the Irganox 1010 stabilizer. Molecular structures for the explosive components are provided in Figure 1. Also included are the structures for the PBX 9501 plasticizers bis(2,2-dinitropopyl)acetal (BDNPA) and bis(2,2-dinitropropyl)formal (BDNPF) as well as Irganox 1010.

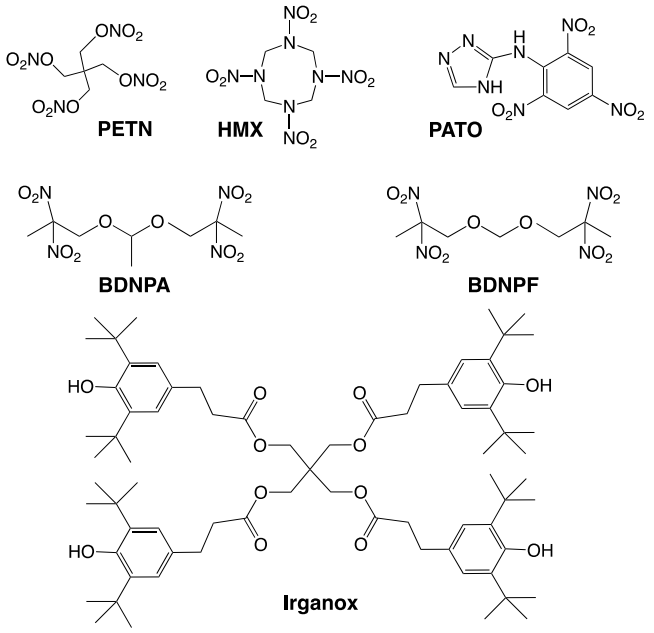

Figure 1. Molecular structures of the molecules of interest used in this study. HMX, BDNPA, BDNPF, and Irganox 1010 are all present in PBX 9501.

PETN is a powerful explosive used commonly throughout military, mining, and even medical applications.[23−25] Previous irradiation studies revealed the formation of multiple gas products that indicated significant degradation of the nitrate ester energetic functional groups.[5,10] Electron paramagnetic resonance (EPR) measurements revealed the formation of several long-lived radical species upon irradiation, including the NO_2 radical[8] and a species tentatively assigned to the PETN radical cation.[15] Investigations into the thermal properties upon irradiation showed a general shift of the endotherms and exotherms to lower temperatures, indicating a potential increase in the ability of an explosive to initiate under typical handling scenarios, otherwise known as the handling sensitivity.[12] These results are further confirmed by measurements to changes in impact sensitivities, a test that directly measures the susceptibility of explosive initiation to an impact insult,[26−29] which showed a general increase in sensitivity as the dose increased.[12,15] Additionally, a study conducted on the shock sensitization showed an increase upon irradiation with a threshold dose of 5 kGy.[30] Overall, previous results suggest that the ionizing radiation degrades PETN and increases the handling sensitivity to some degree.

PBX 9501 is an HMX-based explosive formulation that includes several binders, plasticizers, and the radical scavenger Irganox 1010.[31] Although no radiation aging studies exist on PBX 9501, several studies do exist on the explosive component, HMX. As with PETN, analysis of radiolytically produced gas indicates degradation of the nitramine energetic functional group in addition to the organic structural backbone.[5,6] EPR measurements confirm the formation of the NO_2 radical,[7,9] and X-ray photoelectron spectroscopy (XPS) measurements show an overall loss of NO_2 as a result of irradiation.[16] Interestingly, although radiation appears to lead to a loss of the energetic functional group, HMX also shows an increase in impact sensitivity following irradiation[7,9,12,15] though results also suggest a threshold dose of approximately 7 kGy.[13] Thermal analyses are in line with both observations.[12,13] Studies conducted on Estane 5703, a poly(ester urethane) binder used to decrease mechanical sensitivity in PBX 9501,[32] have found both cross-linking[33] and scission[34] as well as several radical species such as peroxy and nitroxide radicals.[35,36] Irganox 1010, on the other hand, has been found to hinder radiation-induced cross-linking when combined with plastics,[37,38] which is likely due to its function as a radical scavenger. It is possible that Irganox 1010 will offer similar radiation protection to Estane 5703 though the extent of this protection and the resulting effects on the properties of PBX 9501 are not known.

PATO is a high-density, high thermal stability, and low handling sensitivity HE that is gaining renewed interest as a possible replacement for triaminotrinitrobenzene (TATB).[39] Very little data exist for PATO in general, and this study is the first known radiation aging investigation of PATO.

RESULTS AND DISCUSSION

Radiolytic Gas Production. During irradiation, bonds can be broken and gas can be released from solid materials. Based on the chemical composition of the HEs in this study, the main radiolytic gases expected as a result of radiolysis are simple gases composed of hydrogen, nitrogen, oxygen, and carbon. In particular, previous studies indicate that the main gases are expected to be H_2, N_2, N_2O, NO, CO, and CO_2.[5,6] The results from a few selected gases measured in the PBX 9501 samples are shown in Figure 2. The headspace gas from the PATO

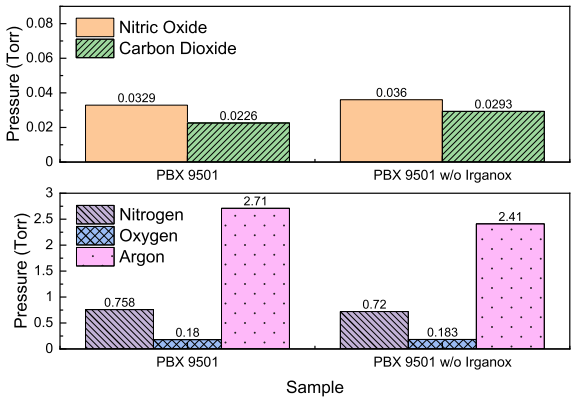

Figure 2. Partial pressures of gases measured after irradiation. The top graph shows the minor components of headspace gases, while the bottom graph shows the major components of headspace gases.

sample was lost due to burst disc failure during the initial evacuation for post-irradiation gas chromatography−mass spectrometry (GC−MS) analysis and thus those results could not be collected. Based on the similarity of the N_2, O_2, and argon ratios seen in the headspace gas of the PETN sample with atmospheric air, it was clear that PETN had developed a leak at some point during the experiment (see Figure S1) though the CO_2 and NO results indicate that not all of the radiolytically produced gas had escaped.

https://doi.org/10.1021/acsomega.1c05703
ACS Omega 2022, 7, 2842−2849

Carbon dioxide (CO_2) is present in air, but the amount is significantly lower than what was measured in any of the samples. A majority of what was measured must therefore come from the radiolysis of the HEs. The amount of measured nitric oxide (NO) is similarly not explainable by atmospheric concentrations, so it too must be a major product from radiolysis. The ratio of nitrogen gas with these gases can therefore give a rough idea of the internal vessel environment. The ratio of CO_2 and NO can also give a quick comparison to previously reported gas measurements. These ratios are listed in Table 1.

Table 1. Radiolytic Gas Ratio Comparisons

	ratios of major gaseous products		
sample	N_2/NO	N_2/CO_2	NO/CO_2
PBX 9501	23.0	33.5	1.5
PBX 9501 w/o irganox	20.0	24.6	1.2
HMX[6]	3.2	6.4	2.0
HMX[5]	5.0	5.7	1.1
PETN	84.2	56.2	0.7
PETN[5]	1.3	5.2	4.1

Although there are no studies on the radiolysis of PBX 9501 samples, there have been a few studies on HMX, which is the main component of PBX 9501. The relative ratios should therefore be comparable. For both the PBX 9501 samples used in this study, the relative concentration of nitrogen is significantly larger than what has been reported for HMX. The NO/CO_2 ratios, however, fall within the two previously reported values. These results suggest either that some of the nitrogen gas measured is from air or that there was possibly an impurity from air that was not able to be removed consistently. In either case, it appears that there was an imperfect initial internal vessel environment and possibly incomplete evacuation during the pre-GC injection phase. However, the results also indicate that the imperfect irradiation environment did not have a large effect on the results of the irradiation of the PBX 9501 samples. The irradiation environment is important and different environments can lead to different results.[7,9] The PETN results demonstrate this concept more clearly as the irradiation environment was further from ideal than the PBX 9501 samples. The nitrogen ratios significantly differ from the previously reported values as expected given the results from the left graph in Figure S1. Unlike the PBX 9501 samples, however, the NO/CO_2 ratio is also quite a bit different than the literature value. The displayed literature values for all samples were from irradiation conducted under vacuum.

Physical Changes. Radiolysis produces gas in these materials. If the production rate of gas is larger than the diffusion rate of gas in any of the materials, the gas can buildup and cause the material to expand or even fracture.[5,10,11] The particle size and morphology may have an effect on the small-scale sensitivity measurements of an explosive,[24,29] so it was necessary to investigate any potential changes in the particle size following irradiation. The particle size and morphology were assessed by scanning electron microscopy (SEM).

Both the PBX 9501 samples and the PETN sample were all pressed into pellets prior to irradiation. Though the PETN particle size can coarsen during thermal aging in low-density detonator pellets,[25] there were no discernable changes for PETN or the PBX 9501 samples upon irradiation, as shown in Figure S14. The particle size and morphology for PATO shown in Figure 3 similarly did not change upon irradiation, indicating that the gas production rate was less than the gas diffusion rate within the parameters of this experiment. Due to the low dose rate, this is not an unexpected result.

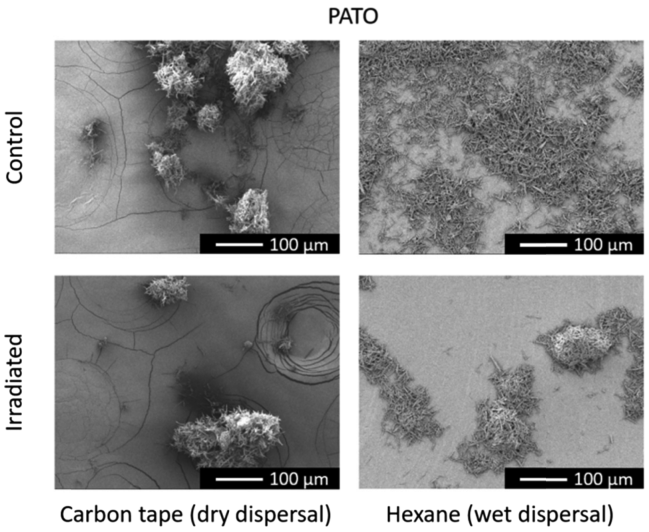

Figure 3. SEM micrographs of control (top) and irradiated (bottom) PATO for both dry dispersal (left) and wet dispersal (right).

Although the particle size and morphology for PATO did not change upon irradiation, an interesting phenomenon was observed in the SEM micrographs, as shown in Figure 3. Typically, PATO forms large aggregate structures as a result of the morphology and synthesis. When using a wet dispersal method for SEM analysis, the dispersion method was sufficient to disrupt these aggregate structures. This concept is demonstrated by looking at both the dry and the wet dispersal micrographs for the control PATO. After irradiation, the wet dispersal method was no longer able to disrupt the aggregates. This result suggests that the surface energy of the powder was altered during irradiation. Interestingly, a previous measurement of the surface activity of HMX upon irradiation found that the surface activity increased as the delivered dose increased.[6] More tests should be conducted to assess potential changes to the surface characteristics of PATO as a result of irradiation.

Bulk Structural Changes. The collected nuclear magnetic resonance (NMR) spectra for both the control and irradiated samples of PETN, shown in Figure S10, were nearly identical with a single peak for PETN (8H, CH_2) at 4.65 ppm.[23] One small singlet (at <1% level) was observed in the aged sample at 3.63 ppm that was not observed in the pure sample. Another peak at 4.63 ppm appeared in the shoulder of the ~4.7 ppm peak, as shown in Figure 4. It is possible that these peaks are due to the ingrowth of pentaerythritol trinitrate (PETriN) whose structure is shown in the top portion of Figure 4; laboratory measurements of PETriN in acetonitrile-d_3 show a singlet (6H, CH_2) at 4.60 ppm, a doublet (2H, CH_2 by OH) at 3.63 ppm, and a triplet (1H, OH) at 3.34 ppm. It has been shown that thermal degradation of PETN involves the rate-determining scission of the nitrate ester ($O-NO_2$) bond, forming a PETN alkoxy radical.[40,41] Under radiation conditions, hydrogen radicals are present in abundance,[19,42] which could allow the formation of the OH functional group in

https://doi.org/10.1021/acsomega.1c05703
ACS Omega 2022, 7, 2842−2849

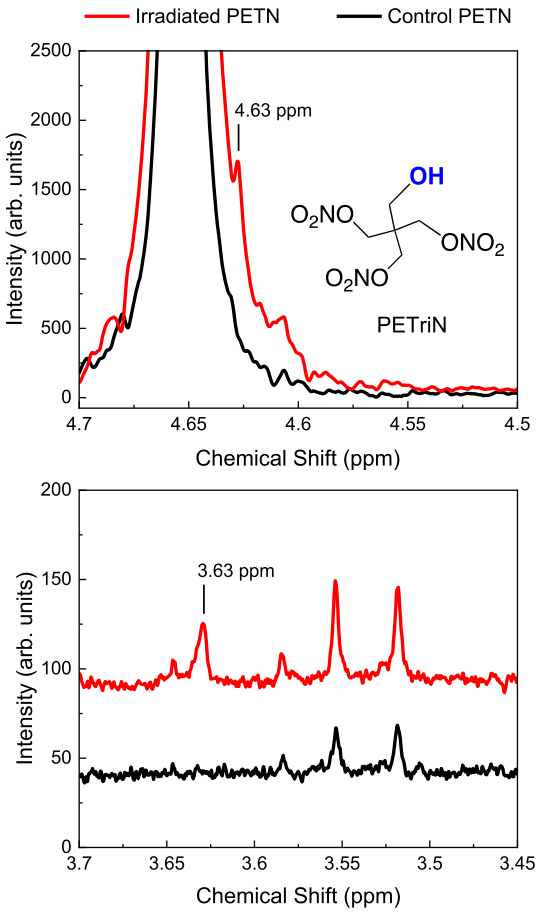

Figure 4. Zoomed-in ^{1}H NMR spectra of irradiated (red line) and control (black line) PETN. The top figure shows the 4.63 ppm peak, while the bottom figure (offset for clarity) shows the 3.63 ppm peak. The structure for PETriN, the suspected species responsible for the new peaks, is also shown in the top figure.

PETriN. Liquid chromatography results should be able to confirm this observation.

NMR spectra of both the control and irradiated samples of PATO in dry dimethyl sulfoxide (DMSO) were identical, with broad peaks at 8.43 (1H), 9.01 (2H), 10.50 (1H), and 13.90 (1H), consistent with the literature values.[39] PBX 9501 samples with and without Irganox 1010 stabilizers were dissolved in DMSO (with no remaining particulates) and all the control and irradiated sample spectra were identical, with a large singlet for HMX at 6.05 ppm (8H, CH_2)[43] and a range of singlets and multiplets observed between 1.2 and 7.4 ppm for the binder system, consistent with the literature values.[44−46] The full ^{1}H NMR results for PETN, PATO, and both PBX 9501 samples are provided in the Supporting Information.

Changes to Explosive Handling Sensitivity. A major concern for irradiated HEs is the potential for influencing handling sensitivity characteristics. Drop-weight impact tests estimate explosive sensitivity by measuring the drop height required for a sample to react with 50% probability; this number is referred to as the H_{50} value. These tests are some of the most common methods for measuring handling sensitivity using a small-scale test. The impact results for this study are provided in Table 2. The uncertainty listed in the table is the calculated standard deviation from 15 drops used to compute H_{50}.

Table 2. Drop Heights for Control and Irradiated HEs

	H_{50} (cm)	
sample	control	irradiated
PBX 9501	35.7 ± 2.9	31.4 ± 2.1
PBX 9501 w/o irganox	33.5 ± 5.3	32.9 ± 3.3
PATO	>320	>320
PETN	18.0 ± 1.7	14.2 ± 2.0

Although all measureable H_{50} values were smaller for the irradiated material than those for the control material, the values are not statistically different. No discernable changes were seen in the differential scanning calorimetry (DSC) results (see Supporting Information), which further confirms the lack of increase in sensitivity upon irradiation. These results agree with previous studies that showed no discernable difference in HEs irradiated under nonvacuum conditions to a dose of 7 kGy,[13] 3.5 times the dose used in this study. Some previous studies[7,9,12−14] have found that ionizing radiation can increase an explosive's sensitivity to impact, making the explosive more sensitive, but those studies utilized larger doses and dose rates than used in this study. Additionally, previous studies reveal that the irradiation environment plays a key part in the post-irradiation drop height results. These results indicate that HEs irradiated under vacuum become more sensitized than HEs irradiated under ambient conditions.[7−9] The prevailing theory is that oxygen reacts with surface radicals to form peroxy radicals.[7] These peroxy radicals would then be more stable to explosive insults and not result in an increase in sensitivity. For this experiment, some amount of air was likely present in all of the vessels though the total amount is unknown. The low total absorbed dose in addition to the presence of oxygen in the irradiation environment can therefore easily explain the impact results seen in this study.

It is currently not known whether an inert gas irradiation atmosphere will show the same increase in sensitivity as that observed for vacuum irradiation. It is possible that the surface degradation could actually be enhanced because of Penning ionization,[47,48] which could lead to more sensitization. Future experiments aim to study this phenomenon to fully understand the effect of the irradiation environment on the sensitization of HEs since the irradiation environment for explosives in the stockpile or on space shuttles likely ranges from typical atmospheric conditions all the way to the vacuum of space.

PATO does not react within the 320 cm drop height range of the LANL impact apparatus but does have a measureable sensitivity to electrostatic discharge (ESD). PATO was therefore tested for changes in ESD sensitivity upon irradiation. Both the more traditional tape method and a new image analysis method were employed. To the authors' knowledge, only two previous tests have been conducted on the ESD behavior of HEs upon irradiation. One study was conducted on a PBX formulation involving TATB that was aged in the stockpile for over 7 years and it revealed no change in behavior as a result of irradiation.[17] The other study was conducted on pure TATB and it revealed a significant change to higher sensitivity following a dose of 50 kGy.[18]

When using the more traditional tape method, the control PATO had a threshold of initiation level (TIL) of 0.0625 J, while the irradiated PATO had a TIL of 0.125 J. This difference only represents a single testing level, so the experiment was repeated using a Phantom camera and GoDetect image analysis software. Images from a representa-

https://doi.org/10.1021/acsomega.1c05703
ACS Omega 2022, 7, 2842−2849

tive test for each sample are shown in Figure S15. The results obtained using this method also suggest that the irradiated PATO is less sensitive to ESD than the control PATO. However, the testing TILs are too coarse to claim a significant difference and studies are being conducted to improve the method further. It is possible that these results are related to the change in aggregation behaviors observed in the SEM micrographs though further studies must be conducted to confirm this.

CONCLUSIONS

Understanding the radiation aging of HEs and explosive formulations is important for ensuring their continued safety after exposure to ionizing radiation fields. This study explored the low dose, low dose rate radiation aging of four explosives PETN, PATO, and PBX 9501 both with and without the Irganox 1010 stabilizer. Impact sensitivity and DSC measurements for all samples did not show a significant change upon irradiation. ^{1}H NMR results showed the appearance of two peaks in the irradiated PETN sample that are tentatively attributed to the formation of PETriN, a common decomposition product formed by thermally degrading PETN. Both SEM micrographs and ESD tests suggest a surface energy change in PATO, but more studies must be conducted to confirm this observation. Overall, the radiation aging of the explosives explored in this study did not appear to have significant consequences for the dose and dose rate utilized.

METHODS AND MATERIALS

Materials. PETN powder was obtained from DuPont, processed at the Los Alamos National Laboratory (LANL), and pressed into pellets measuring 7 mm diameter × 2 mm height; the final pressing density was 1.65 g/cm^3. PATO was synthesized at LANL in accordance to a previously published method.[39] PATO cannot be pressed well and was irradiated as a powder. PBX 9501 was formulated at LANL; one batch included Irganox 1010 while the other batch did not include Irganox 1010. The nominal composition of PBX 9501 is 94.9% HMX, 2.5% Estane 5703, 2.5% 1:1 mixture of BDNPA and BDNPF (collectively referred to as BDNPA/F), 0.1% Irganox 1010, and 0.004% *n*-phenyl-naphthylamine.[31] Both batches of PBX 9501 were pressed into pellets measuring 10 mm diameter × 1 mm height and were pressed to ∼98% of the theoretical maximum density of 1.86 g/cm^3.

Sample Preparation and Irradiation. Prior to irradiation, approximately 0.5−2 g of the material was placed into Pyrex ampoules hermetically bonded to stainless steel conflat flanges (Accu-Glass). PETN and PATO were contained within 1.33-inch diameter glass ampoules, while the PBX 9501 samples were contained within 2.75-inch diameter glass ampoules. The material was placed into the glass ampoules, flushed with argon gas for approximately 10 min, and then sealed with a 10−11 psig burst disc (Accu-Glass). The combination of the sealed glass ampoule with the burst disc was then referred to as the irradiation vessel or simply vessel. The nominal volume was 60 mL for the smaller diameter vessels and 190 mL for the larger diameter vessels. After being sealed via the conflat flange, the samples were placed into seamless steel pipes to meet the U.S. Department of Transport (DOT) standards for transportation of explosives and shipped to the Sandia National Laboratories (SNL). Once at SNL, the vessels were repackaged into ammo cans for irradiation.

Irradiation took place at the Low Dose Rate Irradiation Facility (LDRIF) located at SNL. The ammo cans were stacked two high and arranged in an arc around the ^{137}Cs (E_γ = 662 keV) source. The dose rate was measured in the ammo can using thermoluminescence detectors and determined to be approximately 0.127 Gy/h with respect to calcium fluoride (CaF_2). The vessels were kept at the LDRIF for almost 22 months to achieve an absorbed dose of 2 kGy. A visual representation of the irradiation setup is provided in Figure S16.

Analyses. Following irradiation, several analyses were conducted to assess the radiation-induced changes to the materials. Analyses were also concurrently conducted on the unirradiated (control) materials for comparison.

Headspace gas was collected and analyzed using an Agilent 7890A gas chromatograph (GC) fitted with an Agilent 5975C mass spectrometer (MS). A custom holder was designed to fit over the burst disc of each vessel. The space above the burst disc was first evacuated to remove the atmospheric gas. The burst disc was then punctured, and the gas was injected into the GC−MS. Gas was injected at a split ratio of 10:1 into an Agilent PoraBOND Q column (30 m × 250 μm × 5 μm film thickness). Ultrahigh purity helium was used as the carrier gas with a flow of 1.2 mL/min. The oven on the MS was started at an initial temperature of −60 °C to allow for the separation of the permanent gases, and then the temperature of the oven was ramped to 175 °C at a rate of 10 °C/min where it was held for 1 min. The oven temperature was then ramped to 200 °C at a rate of 10 °C/min where it was held for an additional 0.5 min. The injection temperature was 280 °C. No solvent delay was used, and a mass range of 10−550 amu *m*/*z* was scanned to monitor gas species with the MS detector. The gases analyzed were nitrogen, oxygen, argon, carbon monoxide, NO, CF_4, methane, CO_2, nitrous oxide, ethylene, ethane, propane, and isobutylene. The number of injections was based on the amount of available starting gas, which varied between samples. It is noted that NO is a reactive gas and can be difficult to measure and quantify with a GC−MS. The GC was calibrated with a four-point calibration using a standard calibration gas of 10% NO in helium. The calibration curve had a linear correlation factor of >0.995; this result in addition to daily calibration checks indicates that the process is in control and the numbers are valid.

Physical changes were assessed using an SEM. The SEM analysis was carried out using a JEOL 7900F field-emission microscope with a Schottky Plus electron gun. The analytical resolution was <30 nm. Samples made from pellets were gently crushed in a liquid N_2 bath to reduce the likelihood of initiation. A small piece was then mounted to an aluminum SEM stub using conductive carbon tape. PATO was irradiated as a powder and therefore prepared in both wet dispersal and dry dispersal methods. For the wet dispersal, a small amount of PATO was deposited onto an aluminum SEM stub. A few drops of hexane were added to the stub and a spatula was used to disperse the powder. This method resulted in a roughly uniform distribution of the material that had good electrical contact with the SEM stub. The dry dispersal method involved tapping a small amount of material onto conductive carbon tape and knocking off excess powder. Once mounted, all samples were sputter-coated with 8 nm of Au/Pd (80:20) to reduce charging during imaging.

Bulk structural changes were measured by NMR spectroscopy, which was estimated to provide information on

https://doi.org/10.1021/acsomega.1c05703
ACS Omega 2022, 7, 2842−2849

decomposition products at the ∼1% level. ^{1}H NMR spectra were recorded using a 400 MHz Bruker spectrometer, and NMR signals were referenced to residual solvent signals in the deuterated solvents. PETN samples were collected in dry acetonitrile-d_3, PATO samples were collected using dry DMSO-d_6, and PBX 9501 samples were collected with benchtop DMSO-d_6. There was no indication of undissolved material in the NMR samples.

Small-scale sensitivity was assessed using impact sensitivity testing, and for PATO, electrostatic discharge (ESD) testing was employed. The nominal humidity at the time of the small-scale sensitivity tests was 40%, and the temperature was about 22 °C. Impact testing was conducted using an ERL Type 12 Impact testing apparatus. Approximately 40 mg of HE was placed on a 150 grit sandpaper circle. This was then placed between an anvil and a striker, both made of hardened steel. A 2.5 kg drop weight was suspended using an electromagnet, and the height was controlled with a pulley system. Two microphones placed in close proximity to the instrument were set up to trigger for sounds >90 dB, and the impact was considered an initiation event if the average of the two microphone sounds was above 117 dB. Approximately 15 impact test trials were completed on each sample and the results of these drops were analyzed using the Neyer D-Optimal method[49] to obtain the height at which there is a 50% chance of initiation (H_{50}).

ESD was conducted using an ABL electrostatic discharge apparatus. Approximately 5 mg of HE was used for each ESD test, which used a charging voltage of 500 VDC. Energy was delivered to the sample by quickly lowering a sharp tip, which then discharged the capacitor selected from a bank using the rotary switch. This setup could deliver energies of 0.25, 0.125, 0.0625, or 0.025 J. Two different ESD testing methods were employed in this study: the more traditional tape method and image analysis software coupled with a camera. For the tape method, HE was deposited in a well in the center of a Teflon disc (∼0.6 cm diameter and 0.4 cm depth) that had a hardened steel bottom. The HE was distributed such that the hardened steel bottom was completely covered, and the well was completely covered using Magic tape from Scotch. After the needle was retracted, the tape was inspected for any rupturing in addition to the perforation from the needle itself, which would be considered an initiation event. Once an initiation was determined at one energy level, the next level down was tested. This method was repeated until a level had 13 consistent trials with no tape rupturing, which was then reported as the ESD test value. The computer-assisted method used a slightly different sample holder that did not contain a well. Instead, the hardened steel disc was level with the Teflon holder disc. A high-speed Phantom camera was centered with the HE in view and set up to take a series of four pictures triggered by the lowering of the needle. The pictures were then analyzed by the image analysis software GoDetect developed by Safety Management Services, Inc. (godetect.smsenergetics.com). The software would analyze the Phantom images and determine the probability that the event was a no go, a minor go (1−5 ppm of CO evolved), a significant go (5−20 ppm of CO evolved), or an extreme go (>20 ppm of CO evolved). Each energy level was tested three times and the highest energy with a no go result was reported as the ESD value.

Thermal properties were also measured using a DSC. DSC measurements were conducted using a Q2000 from TA Instruments. Approximately 1 mg of HE was heated from 50 to 450 °C at a ramp rate of 10 °C/min in a hermetic aluminum crucible with an aluminum lid containing a pinhole. Ultrahigh purity N_2 gas was flowed at a rate of 50 mL/min during the run. An empty pan was run before the HE samples and subtracted out from the sample measurements. An indium standard measurement was also run to ensure that the instrument was operating as expected.

■ ASSOCIATED CONTENT

Supporting Information

The Supporting Information is available free of charge at https://pubs.acs.org/doi/10.1021/acsomega.1c05703.

PETN GC−MS results, DSC results, NMR results, SEM micrographs of pellets, GoDetect results, and irradiation configuration (PDF)

■ AUTHOR INFORMATION

Corresponding Author

Virginia W. Manner − *High Explosives Science and Technology, Los Alamos National Laboratory, Los Alamos, New Mexico 87545, United States;* orcid.org/0000-0002-1916-4887; Email: vwmanner@lanl.gov

Authors

Patricia L. Huestis − *High Explosives Science and Technology, Los Alamos National Laboratory, Los Alamos, New Mexico 87545, United States;* orcid.org/0000-0002-1863-2757

Jamie A. Stull − *High Explosives Science and Technology, Los Alamos National Laboratory, Los Alamos, New Mexico 87545, United States;* Present Address: Finishing and Manufacturing Science, Los Alamos National Laboratory, Los Alamos, New Mexico 87545, United States (J.A.S.)

Joseph P. Lichthardt − *High Explosives Science and Technology, Los Alamos National Laboratory, Los Alamos, New Mexico 87545, United States*

Maryla A. Wasiolek − *Gamma Irradiation Facility, Sandia National Laboratories, Albuquerque, New Mexico 87123, United States*

Lori Montano-Martinez − *Energetic Materials, Sandia National Laboratories, Albuquerque, New Mexico 87123, United States*

Complete contact information is available at: https://pubs.acs.org/10.1021/acsomega.1c05703

Author Contributions

P.L.H. was involved in writing the original draft, conceptualization, visualization, and investigation. J.A.S. was involved in design and conceptualization. J.P.L. was involved in design. M.A.W. was involved in investigation. L.M.-M. was involved in investigation. V.W.M. was involved in writing, reviewing, and editing the manuscript, conceptualization, investigation, and supervision.

Notes

The authors declare no competing financial interest.

■ ACKNOWLEDGMENTS

The authors would like to thank Lisa M. Klamborowski, Danielle Montanari, Hongzhao Tian, and Geoffrey W. Brown for impact/ESD tests, SEM analysis, DSC analysis, and analytical discussions, respectively. We also thank Ernie Hartline for formulating the PBX 9501 samples, Philip

Leonard for synthesizing the PATO, and John Kramer for processing the PETN. We thank Dan McDonald for help in preparing the irradiation vessels. The irradiation vessels were based on a design by Douglas Safarik who provided incredibly helpful discussions with regard to the design. We acknowledge the work that Lee Stauffacher and Don Hanson of SNL did to progress the irradiation of HE at Sandia irradiation facilities. This work was supported by the US Department of Energy through the Los Alamos National Laboratory. Los Alamos National Laboratory is operated by Triad National Security, LLC, for the National Nuclear Security Administration of U.S. Department of Energy (Contract No. 89233218CNA000001). The authors would like to thank the LANL Aging and Lifetimes Program for funding as well as Sheldon Larson and Charles Hills for their helpful discussion throughout the entirety of this project. This contribution is LA-UR-21-29428 from Los Alamos National Laboratory.

■ ABBREVIATIONS

BDNPA	bis(2,2-dinitropropyl)acetal
BDNPF	bis(2,2-dinitropropyl)formal
DMSO	dimethyl sulfoxide
DOT	Department of Transportation
DSC	differential scanning calorimetry
EPR	electron paramagnetic resonance
ESD	electrostatic discharge
GC−MS	gas chromatography−mass spectrometry
HE	high explosives
HMX	1,3,5,7-tetranitro-1,3,5,7-tetrazoctane
LANL	Los Alamos National Laboratory
LDRIF	Los Dose Rate Irradiation Facility
NMR	nuclear magnetic resonance
PATO	3−picrylamino−1,2,4−triazole
PBNA	*n*-phenyl-naphthylamine
PBX	plastic-bonded explosive
PETN	pentaerythritol tetranitrate
PETriN	pentaerythritol trinitrate
SEM	scanning electron microscopy
SNL	Sandia National Laboratories
TATB	triaminotrinitrobenzene
TIL	threshold of initiation level
TLD	thermoluminescent dosimeter
TMD	theoretical maximum density
XPS	X-ray photoelectron spectroscopy

■ REFERENCES

(1) Lake, E. R., Thompson, S. J., Drexelius, V. W. *A Study of the Role of Pyrotechnic Systems on the Space Shuttle Program*, Report NASA CR-2292, St. Louis, MO, 1973.
(2) Manaa, M. R.; Mitchell, A. R.; Garza, R. G.; Pagoria, P. F.; Watkins, B. E. Flash Ignition and Initiation of Explosives−Nanotubes Mixture. *J. Am. Chem. Soc.* **2005**, *127*, 13786−13787.
(3) Glavier, L.; Nicollet, A.; Jouot, F.; Martin, B.; Barberon, J.; Renaud, L.; Rossi, C. Nanothermite/RDX-Based Miniature Device for Impact Ignition of High Explosives. *Propellants, Explos., Pyrotech.* **2017**, *42*, 308−317.
(4) Benton, E. R.; Benton, E. V. Space Radiation Dosimetry in Low-Earth Orbit and Beyond. *Nucl. Instrum. Methods Phys. Res. B* **2001**, *184*, 255−294.
(5) Urizar, M. J.; Loughran, E. D.; Smith, L. C. *The Effects of Nuclear Radiation on Organic Explosives*, Report TID-12491, Los Alamos, New Mexico, 1960
(6) Castorina, T. C.; Haberman, J.; Smetana, A. F. Radiation-Enhanced Surface Activity of an Organic Explosive, γ-HMX. *Int. J. Appl. Radiat. Isot.* **1968**, *19*, 495−503.
(7) Miles, M. H.; DeVries, K. L.; Britt, A. D.; Moniz, W. B. Impact Sensitivity of γ-Irradiated HMX. *Propellants, Explos., Pyrotech.* **1983**, *8*, 49−52.
(8) Miles, M. H.; Devries, K. L. Free Radicals in γ-Irradiated PETN. *J. Mater. Sci.* **1984**, *19*, 467−472.
(9) Miles, M. H.; Devries, K. L.; Britt, A. D.; Moniz, W. B. Generation of Free Radicals in RDX and HMX Compositions. *Propellants, Explos., Pyrotech.* **1982**, *7*, 100−106.
(10) Rosenwasser, H.; O. R. N. Laboratory; U. S. A. E. Commission. *Effects of Gamma Radiation on Explosives: Final and Summary Report on Army Ordnance Project TA3-5003R*; Oak Ridge National Laboratory: Oak Ridge, TN, 1955.
(11) Mapes, J. E.; Schwartz, F. R.; Kaufman, J. V. R.; Levy, P. W. *Effects of Gamma-Ray Irradiation on Five Plastic-Bonded High Explosive Compositions*; Brookhaven National Laboratory Supported By Picatinny Arsenal: Brookhaven, NY, 1962.
(12) Avrami, L.; Jackson, H. J.; Kirshenbaum, M. S. *Radiation-Induced Changes in Explosive Materials*, Report 4602; Picatinny Arsenal: Wharton, NJ, 1973.
(13) Avrami, L.; Jackson, H. J. *Effect of Long Term Low-Level Gamma Radiation on Thermal Sensitivity of RDX-HMX Mixtures*, Report 4964; Picatinny Arsenal: Wharton, NJ, 1976.
(14) Lewis, D.; Padfield, J.; Connors, S.; Wilson, I.; Akhavan, J. Further Insights into the Discoloration of TATB under Ionizing Radiation. *J. Energ. Mater.* **2020**, *38*, 362−376.
(15) Lewis, D. *The Effect of Ionising Radiation on the Explosives: TATB, HMX and PETN*; Cranfield University, 2019.
(16) Beard, B. C.; Sharma, J. The Radiation Sensitivity of NTO (3-Nitro-1,2,4-Triazol-5-One). *J. Energ. Mater.* **1989**, *7*, 181−198.
(17) Skidmore, C. B.; Idar, D. J.; Buntain, G. A.; Son, S. F.; Sander, R. K. Aging and PBX 9502. In *Conference on life cycles of energetic materials*, Fullerton, CA (United States) , 1998.
(18) Connors, S. *The Effects of Gamma Radiation on a PBX Containing TATB and the Fluoropolymer FK-800*; Cranfield University, 2014.
(19) Voevodskii, V. V.; Molin, Y. N. On The Radiation Stability of Solid Organic Compounds. *Radiat. Res.* **1962**, *17*, 366.
(20) Chang, Z.; Laverne, J. A. Dynamic Evolution of Gases in the γ- and Helium-Ion Radiolyses of Solid Polymers. *J. Polym. Sci. B Polym. Phys.* **2001**, *39*, 1449−1459.
(21) Price, D. Contrasting Patterns in the Behavior of High Explosives. *Symp. Combust.* **1967**, *11*, 693−702.
(22) Cooper, P. W. *Explosives Engineering*; Wiley-VCH Verlag, 2018.
(23) Binks, P. R.; French, C. E.; Nicklin, S.; Bruce, N. C. Degradation of Pentaerythritol Tetranitrate by Enterobacter Cloacae PB2. *Appl. Environ. Microbiol.* **1996**, *62*, 1214−1219.
(24) Foltz, M. F. *Aging of Pentaerythritol Tetranitrate (PETN)*, Report LLNL-TR-415057; Lawrence Livermore National Laboratory: Livermore, CA, 2009.
(25) Lease, N.; Burnside, N. J.; Brown, G. W.; Lichthardt, J. P.; Campbell, M. C.; Buckley, R. T.; Kramer, J. F.; Parrack, K. M.; Anthony, S. P.; Tian, H.; Sjue, S. K.; Preston, D. N.; Manner, V. W. The Role of Pentaerythritol Tetranitrate (PETN) Aging in Determining Detonator Firing Characteristics. *Propellants, Explos., Pyrotech.* **2021**, *46*, 26−38.
(26) Sandstrom, M. M.; Brown, G. W.; Preston, D. N.; Pollard, C. J.; Warner, K. F.; Sorensen, D. N.; Remmers, D. L.; Phillips, J. J.; Shelley, T. J.; Reyes, J. A.; Hsu, P. C.; Reynolds, J. G. Variation of Methods in Small-Scale Safety and Thermal Testing of Improvised Explosives. *Propellants, Explos., Pyrotech.* **2015**, *40*, 109−126.
(27) Rae, P. J.; Dickson, P. M. Some Observations About the Drop-Weight Explosive Sensitivity Test. *J. Dyn. Behav. Mater.* **2021**, *7*, 414−424.
(28) Marrs, F. W.; Manner, V. W.; Burch, A. C.; Yeager, J. D.; Brown, G. W.; Kay, L. M.; Buckley, R. T.; Anderson-Cook, C. M.; Cawkwell, M. J. Sources of Variation in Drop-Weight Impact

https://doi.org/10.1021/acsomega.1c05703
ACS Omega 2022, 7, 2842−2849

Sensitivity Testing of the Explosive Pentaerythritol Tetranitrate. *Ind. Eng. Chem. Res.* **2021**, *60*, 5024−5033.
(29) Lease, N.; Holmes, M. D.; Englert-Erickson, M. A.; Kay, L. M.; Francois, E. G.; Manner, V. W. Analysis of Ignition Sites for the Explosives 3,3′-Diamino-4,4′-Azoxyfurazan (DAAF) and 1,3,5,7-Tetranitro-1,3,5,7-Tetrazoctane (HMX) Using Crush Gun Impact Testing. *ACS Mater. Au* **2021**, *1*, 116.
(30) Dick, J. J. Plane Shock Initiation of Detonation in Γ-irradiated Pentaerythritol Tetranitrate. *J. Appl. Phys.* **1982**, *53*, 6161−6167.
(31) Freye, C. E.; Rosales, C. J.; Thompson, D. G.; Brown, G. W.; Larson, S. A. Development of Comprehensive Two-Dimensional Liquid Chromatography for Investigating Aging of Plastic Bonded Explosives. *J. Chromatogr. A* **2020**, *1611*, No. 460580.
(32) Orler, E. B.; Wrobleski, D. A.; Smith, M. E. Hydrolytic Degradation of Estane 5703. In *22nd Aging Compatibility and Stockpile Stewardship Conference*, Oak Ridge, TN (US), 1999.
(33) Tian, Q.; Takács, E.; Krakovský, I.; Horváth, Z. E.; Rosta, L.; Almásy, L. Study on the Microstructure of Polyester Polyurethane Irradiated in Air and Water. *Polymers* **2015**, *7*, 1755.
(34) Pierpoint, S.; Silverman, J.; Al-Sheikhly, M. Effects of Ionizing Radiation on the Aging of Polyester Based Polyurethane Binder. *Radiat. Phys. Chem.* **2001**, *62*, 163−169.
(35) Cooke, D. W.; Muenchausen, R. E.; Bennett, B. L.; Orler, E. B.; Wrobleski, D. A.; Smith, M. E.; Jahan, M. S.; Thomas, D. E. Luminescence, Optical Absorption and Electron Spin Resonance of an X-Irradiated Poly(Ester Urethane). *Radiat. Phys. Chem.* **1999**, *55*, 1−13.
(36) Jahan, M. S.; Thomas, D. E.; King, M. C.; Cooke, D. W.; Bennett, B. L.; Orler, E. B.; Wrobleski, D. A. Electron Spin Resonance Study of Oxidation in X-Irradiated Poly(Ester Urethane) Containing Nitroplasticizer. *Nucl. Instrum. Methods Phys. Res. B* **2001**, *185*, 351−354.
(37) Ratnam, C. T.; Nasir, M.; Baharin, A.; Zaman, K. Electron-Beam Irradiation of Poly(Vinyl Chloride)/Epoxidized Natural Rubber Blend in the Presence of Irganox 1010. *Polym. Degrad. Stab.* **2001**, *72*, 147−155.
(38) Ratnam, C. T.; Nasir, M.; Baharin, A. Irradiation Crosslinking of Unplasticized Polyvinyl Chloride in the Presence of Additives. *Polym. Test.* **2001**, *20*, 485−490.
(39) Leonard, P.; Bowden, P.; Shorty, M.; Schmitt, M. Synthesis and Evaluation of 3-Picrylamino-1,2,4-Triazole (PATO) Formulations. *Propellants, Explos., Pyrotech.* **2019**, *44*, 203−206.
(40) Chambers, D. M.; Brackett, C. L.; Sparkman, O. D. *Perspectives on Pentaerythritol Tetranitrate (PETN) Decomposition*, Report UCRL-ID-148956; Lawrence Livermore National Laboratory: Livermore, CA, 2002.
(41) Roos, B. D.; Brill, T. B. Thermal Decomposition of Energetic Materials 82. Correlations of Gaseous Products with the Composition of Aliphatic Nitrate Esters. *Combust. Flame* **2002**, *128*, 181−190.
(42) Dewhurst, H. A. Radiation Chemistry of Organic Compounds. I. n-Alkane Liquids. *J. Phys. Chem.* **1957**, *61*, 1466−1471.
(43) Zhang, Y.; Xu, Z.; Ruan, J.; Wang, X.; Zhang, L.; Luo, J. A Stepwise Strategy for the Synthesis of HMX from 3,7-Dipropionyl-1,3,5,7-Tetraazabicyclo[3.3.1]Nonane. *Propellants, Explos., Pyrotech.* **2018**, *43*, 1287−1295.
(44) Jayawickrama, D. A.; Larive, C. K.; McCord, E. F.; Roe, D. C. Polymer Additives Mixture Analysis Using Pulsed-Field Gradient NMR Spectroscopy. *Magn. Reson. Chem.* **1998**, *36*, 755−760.
(45) LeMaster, D. M.; Hernández, G. NMR Analysis of Polyester Urethane End Groups and Solid-Phase Hydrolysis Kinetics. *Macromolecules* **2000**, *33*, 3569−3576.
(46) Désilets, S.; Perreault, F. Comparative Study of Two Methods Used for the Characterization of the Degradation of the Polymer Binder in Gap-Based Propellants. *J. Energ. Mater.* **1997**, *15*, 109−124.
(47) Parker-Quaife, E. H.; Verst, C.; Heathman, C. R.; Zalupski, P. R.; Horne, G. P. Radiation-Induced Molecular Hydrogen Gas Generation in the Presence of Aluminum Alloy 1100. *Radiat. Phys. Chem.* **2020**, *177*, No. 109117.
(48) Parker-Quaife, E. H.; Horne, G. P. *Milestone 2.8 : Preliminary Radiolytic Gas Generation Measurements from Helium - Backfilled Samples*, Report INL/EXT-21-61404-Rev000; Idaho National Laboratory: Idaho Falls, ID, 2020.
(49) Never, B. T. AD-Optimality-Based Sensitivity Test. *Technometrics* **1994**, *36*, 61−70.

https://doi.org/10.1021/acsomega.1c05703
ACS Omega 2022, 7, 2842−2849